

### Heat generating porous matrix effects on Brownian motion of nanofluid

Zehforoosh, Aydin; Hossainpour, Siamak; Rashidi, Mohammad Mehdi

DOI:

[10.1108/HFF-02-2018-0068](https://doi.org/10.1108/HFF-02-2018-0068)

License:

None: All rights reserved

*Document Version*

Peer reviewed version

*Citation for published version (Harvard):*

Zehforoosh, A, Hossainpour, S & Rashidi, MM 2018, 'Heat generating porous matrix effects on Brownian motion of nanofluid', International Journal of Numerical Methods for Heat & Fluid Flow. <https://doi.org/10.1108/HFF-02-2018-0068>

[Link to publication on Research at Birmingham portal](#)

#### **Publisher Rights Statement:**

Citation: Zehforoosh, Aydin, Siamak Hossainpour, and Mohammad Mehdi Rashidi. "Heat generating porous matrix effects on Brownian motion of nanofluid." International Journal of Numerical Methods for Heat & Fluid Flow

Published in International journal of Numerical Methods for Heat and Fluid Flow on 29/10/2018

DOI: <https://doi.org/10.1108/HFF-02-2018-0068>

#### **General rights**

Unless a licence is specified above, all rights (including copyright and moral rights) in this document are retained by the authors and/or the copyright holders. The express permission of the copyright holder must be obtained for any use of this material other than for purposes permitted by law.

- Users may freely distribute the URL that is used to identify this publication.
- Users may download and/or print one copy of the publication from the University of Birmingham research portal for the purpose of private study or non-commercial research.
- User may use extracts from the document in line with the concept of 'fair dealing' under the Copyright, Designs and Patents Act 1988 (?)
- Users may not further distribute the material nor use it for the purposes of commercial gain.

Where a licence is displayed above, please note the terms and conditions of the licence govern your use of this document.

When citing, please reference the published version.

#### **Take down policy**

While the University of Birmingham exercises care and attention in making items available there are rare occasions when an item has been uploaded in error or has been deemed to be commercially or otherwise sensitive.

If you believe that this is the case for this document, please contact [UBIRA@lists.bham.ac.uk](mailto:UBIRA@lists.bham.ac.uk) providing details and we will remove access to the work immediately and investigate.

**Heat generating porous matrix effects on Brownian motion  
of nanofluid**

Journal:	<i>International Journal of Numerical Methods for Heat and Fluid Flow</i>
Manuscript ID	HFF-02-2018-0068.R1
Manuscript Type:	Research Article
Keywords:	Nanofluid, Brownian motion, Porous matrix, Dependent internal heat generation, LTNE model

SCHOLARONE™  
Manuscripts

1

2

3

4

5

6

7

8

9

10

11

12

13

14

15

16

17

18

19

20

21

22

23

24

25

26

27

28

29

30

31

32

33

34

35

36

37

38

39

40

41

42

43

44

45

46

47

48

49

50

51

52

53

54

55

56

57

58

59

60

1     **Abstract**

2     In the present study, effect of mounting heat generating porous matrix in a close cavity on the

3     Brownian term of CuO-water nanofluid was studied numerically. Because of presence of heat

4     source in porous matrix, couple of energy equations is solved for porous matrix and nanofluid

5     separately. Thermal conductivity and Viscosity of nanofluid were assumed to be consisting of a

6     static component and a Brownian component that were functions of volume fraction of the

7     nanofluid and temperature. To explain the effect of the Brownian term on the flow and heat fields,

8     different parameters such as heat conduction ratio, interstitial heat transfer coefficient, Rayleigh

9     number, consountration of nanoparticles and porous material porosity were investigated and the

10    obtained results were compared to those of the non-Brownian solution. Results showed that the

11    Brownian term increases the viscosity of nanofluid, so this term affects the velocity and

12    smoothness of streamlines. Furthermore the porous matrix is cooled with higher Nusselt number

13    because of rising thermal conductivity. Besides, the effect of the Brownian term was seen to be

14    greater at low Rayleigh number, low-porosity and small thermal conductivity of the porous matrix.

15    It was further seen that, mounting the porous material into cavity changes the temperature

16    distribution and increases Brownian term effect and heat transfer functionality of the nanofluid. It

17    is noteworthy that due to decrement of thermal conduction in high porosities, the impact of

18    Brownian term drops severely that it is possible to obtain reliable results even in the case of

19    neglecting the Brownian term in these porosities.

20    **Keywords:** Nanofluid, Brownian motion, Porous matrix, Dependent internal heat generation,

21    LTNE model.

22    **1. Introduction**

1

<http://mc.manuscriptcentral.com/hff>

Natural heat transfer through cavities saturated with heat generating porous media is widely investigated due to its extensive applications in the fields of thermal and geothermal energy, heat convection management (due to buried atomic wastes), combustion technology, porous catalysts, soil pollution, exothermic reactions inside porous reactors, and fuel cells performance enhancement (Rashidi, 2012; Ioan, 2016; Alsabery, 2016; Sheremet, 2015; Rashad, 2017; Qiang, 2013; Alsabery, 2017; Sheikholeslami, 2015). Likewise, there is a novel concept known as nanofluids introduced by Choi (1995) has gained a great deal of attention in a wide range of studies to enhance heat transfer rate by higher thermal conductivity of nanofluids compared to the base fluid. Many industrial processes such as catalytic chemistry, medicine, biology and environmental applications have adopted the approaches concerned with nanotechnologies.

To calculate the viscosity and thermal conductivity of nanofluid, Koo- Kleinstreuer (2004) correlation was employed. Results indicated that the Nusselt number increases by increasing the Rayleigh number and volume fraction of nanoparticle. Also, it increases by decreasing Hartmann number. In further attempts, skin friction coefficient and the Nusselt number of nanofluid were investigated over a stretching sheet with transverse magnetic field, thermal radiation and buoyancy effects were studied by Rashidi et al. (2014). They show that the skin friction coefficient values of Cu nanofluid are greater than CuO nanofluid. The reduced Nusselt number values of Cu are less than CuO nanofluid.

MHD natural convection in a heat generating porous enclosure saturated with Cu-water nanofluid has been studied by Rashad et al. (2017) numerically. Increment of volume fraction of Cu nanoparticles causes to decrement of nanofluid circulation. Besides variation of magnetic flow direction in porous cavity increases the average Nusselt number. Aminossadati and Ghasemi (2011) presented a numerically investigation of laminar natural convection in a two-dimensional

square cavity. The natural convection was generated using two pairs of heat source-sink located on the bottom wall of the cavity and CuO-water nanofluid was used acting as working fluid in their study. The main objective of their assessment was to enhance heat transfer at different volume fraction and Rayleigh numbers. The conjugate mixed convection of  $\text{Al}_2\text{O}_3$ -water inside a double lid-driven square cavity with an inner square solid body has been studied by Alsabery et al. (2018). The Buongiorno's model has been utilized which shows that applying  $\text{Al}_2\text{O}_3$  nanoparticles has an evident enhance of heat transfer in this case. The results show in all conditions except high values of Reynolds and Richardson numbers the dimensions of inner square is adversely proportional to heat transfer increment. Rashad et al. (2018) have assessed entropy generation in MHD natural convection flow according to length and location variation of source and sink. Also it was shown that angles 40, 50 and 300 are the best values for heat transfer in all location of heat source. Mansour et al. (2016) numerically studied MHD natural convection in a cavity saturated by nanofluid. The authors have assessed four different cases based on various arrangements of thermal boundary conditions. Rashidi et al. (2011) studied heat transfer in a porous medium with radiation. Homotopy analysis method was used to achieve a complete analytic solution. The velocity and temperature profiles were illustrated and effect of coupling constant, permeability and radiation parameter on heat transfer of micropolar fluid was investigated. Natural convection heat transfer inside the anisotropic porous cavity saturated with micropolar  $\text{Al}_2\text{O}_3$ /water nanofluid has been investigated by Ahmed and Rashad (2016). Increment of volume fraction of micropolar nanofluid causes to heat transfer enhancement noticeably. Moreover increment in permeability ratio of porous medium results in lower circulation and velocity. Beckermann et al. (1987) experimentally and numerically studied on an enclosure partially filled porous material. Obtained results denoted that penetration of fluid to porous section which is function of the multiplication of

Darcy and Rayleigh numbers, so this penetration could totally change the flow and thermal fields. Moreover, Second law of thermodynamic was studied in a porous rotating disk with an electrically incompressible nanofluid in a uniform vertical magnetic field by Rashidi et al. (2013). They considered various parameters like volume fraction of suspended nanoparticles, suction and magnetic parameters on velocity, thermal field and entropy generation. This paper established a calculation method for rotating fluidic systems which utilized the second law of thermodynamics.

Considering the studies performed so far, it is well obvious that, natural convection of nanofluid in porous cavity has been among the hot topics considered by researchers in recent years, with its different aspects investigated by far. Nevertheless, considering the diversity of the contributing parameters and governing equations applied to nanofluids and porous substances, the need for further studies to complement previous works is obvious. In this paper, despite the previous works, the effect of mounting the porous matrix with internal heat generation was investigated on the improvement of variable properties of nanofluid. In this way, the assumption of Koo- Kleinstreuer was utilized. This assumption considered that the properties of the nanofluid are equal to the summation of constant and variable properties. The amount of heat generation inside the chamber is a function of temperature. Furthermore, in order to address imperfections of previous studies regarding the effects of the introduction of the porous matrix on increasing Brownian term of nanofluid and achieving the highest Nusselt number, effective range of porosity, Rayleigh number, volume fraction of suspended nanoparticles, thermal conductivity, and thermal convection coefficient of the porous substance were further assessed. Results of Brownian term and non-Brownian states were calculated and compared to each other by isotherms, streamlines and Nusselt number of them.

## 2. Numerical modeling

## 2.1 Physical model and governing equation

Figure 1 shows the studied problem consists of a square cavity saturated with CuO-water which its length is  $L$ . Non-deformable, isotropic and homogeneous and heat generating square porous matrix by length of  $L/2$  is mounted in center. Meanwhile the generated heat depends on temperature difference. The temperatures of left and right walls are set to temperatures  $T_h$  and  $T_c$  respectively. Furthermore adiabatic and impermeable assumptions are considered for top and bottom boundaries. Density varies based on Boussinesq approximation. Also thermal conductivity and viscosity of nanofluid depend on the volume fraction and temperature. Thermophysical properties of CuO nanoparticles and base fluid are listed in Table 1. Also, Newtonian nanofluid is considered and the flow regime is laminar and incompressible. The nanoparticles are in thermal equilibrium with base fluid (water), but the nanofluid and porous matrix are not thermal-equilibrium. Because of presence of heat source in porous matrix, couple of energy equations are solved for porous matrix and nanofluid separately. For modeling solid block the porosity is assumed to be 0.005 instead of zero. Also, the dimensions of nanoparticles are very small compared to pore size and suspended nanoparticles are not deposited and agglomerated on the porous material (Nield and Kuznetsov, 2009).

A binary parameter  $\delta$  is introduced to combine porous and nanofluid governing equations, which values of zero and one for  $\delta$  are used to categorize nanofluid and porous media regions, respectively.

The dimensionless forms of governing equations are as following (Kayhani et al. 2011; Kim et al. 2001):

$$\frac{\partial U}{\partial X} + \frac{\partial V}{\partial Y} = 0 \quad (1)$$

$$\left(\frac{\delta}{\varepsilon^2} - (\delta - 1)\right) \left[ U \frac{\partial U}{\partial X} + V \frac{\partial U}{\partial Y} \right] = -\frac{\partial P}{\partial X} + \frac{\mu_{nf}}{\rho_{nf} \alpha_f} \left[ \frac{\partial^2 U}{\partial X^2} + \frac{\partial^2 U}{\partial Y^2} \right] + \delta \frac{\mu_{nf}}{\rho_{nf} \alpha_f Da} U \quad (2)$$

$$\begin{aligned} & \left(\frac{\delta}{\varepsilon^2} - (\delta - 1)\right) \left[ U \frac{\partial V}{\partial X} + V \frac{\partial V}{\partial Y} \right] \\ & = -\frac{\partial P}{\partial Y} + \frac{\mu_{nf}}{\rho_{nf} \alpha_f} \left[ \frac{\partial^2 V}{\partial X^2} + \frac{\partial^2 V}{\partial Y^2} \right] + \delta \frac{\mu_{nf}}{\rho_{nf} \alpha_f Da} V + \frac{\beta_{nf}}{\beta_f} Ra_f Pr_f \theta_{nf} \end{aligned} \quad (3)$$

$$U \frac{\partial \theta_{nf}}{\partial X} + V \frac{\partial \theta_{nf}}{\partial Y} = (\delta(\varepsilon - 1) + 1) \frac{\alpha_{nf}}{\alpha_f} \left[ \frac{\partial^2 \theta_{nf}}{\partial X^2} + \frac{\partial^2 \theta_{nf}}{\partial Y^2} \right] + \delta H(\theta_s - \theta_{nf}) \quad (4)$$

$$0 = \delta(1 - \varepsilon) R_k \frac{(\rho c)_f}{(\rho c)_{nf}} \left[ \frac{\partial^2 \theta_s}{\partial X^2} + \frac{\partial^2 \theta_s}{\partial Y^2} \right] + \delta H(\theta_{nf} - \theta_s) + \delta \frac{\alpha_{nf}}{\alpha_f} q \theta_s \quad (5)$$

Where  $\varepsilon$  is the porosity of porous material which values between 0 and 1 relate the porousness of solid matrix and for nanofluid equals to 1. By applying the dimensionless parameters, the following terms can be introduced as (Kayhani, 2011; Teamah, 2012):

$$\begin{aligned} X &= \frac{x}{L}, \quad Y = \frac{y}{L}, \quad U = \frac{uL}{\alpha_f}, \quad V = \frac{vL}{\alpha_f}, \quad Da = \frac{K}{L^2}, \quad Pr_f = \frac{\nu_f}{\alpha_f} \\ H &= \frac{hL^2}{(\rho c)_{nf} \alpha_f}, \quad R_k = \frac{k_s}{k_f}, \quad P = \frac{pL^2}{\rho_{nf} \alpha_f^2}, \quad \theta_f = \frac{T_f - T_c}{T_h - T_c} \\ \theta_s &= \frac{T_s - T_c}{T_h - T_c}, \quad Ra_f = \frac{g \beta_f L^3 (T_h - T_c)}{\nu_f \alpha_f}, \quad q = \frac{Q_0 L^2}{(\rho c)_{nf} \alpha_{nf}} \end{aligned} \quad (6)$$

By assuming spherical based porous matrix, permeability of porous media can be defined by Organ equation (1952):

$$K = \frac{d^2 \varepsilon^3}{175(1 - \varepsilon^2)} \quad (7)$$

Also the properties of nanofluid can be formulated as below (Khanafer, 2003):



$$\rho_{nf} = \varphi \rho_p + (1 - \varphi) \rho_f \quad (8)$$

$$(\rho c)_{nf} = \varphi (\rho c)_p + (1 - \varphi) (\rho c)_f \quad (9)$$

$$(\rho \beta)_{nf} = \varphi (\rho \beta)_p + (1 - \varphi) (\rho \beta)_f \quad (10)$$

Based on Koo- Kleinstreuer (2004; 2005) equations, Viscosity and conductivity of nanofluid is formulated as summation of constant static part and variable Brownian part:

$$\mu_{nf} = \mu_{Static} + \mu_{Brownian} \quad (11)$$

$$k_{nf} = k_{Static} + k_{Brownian} \quad (12)$$

The Brinkman (1952) and Maxwell–Garnett’s (1904) model is utilized to expressing static viscosity and thermal conductivity respectively:

$$\mu_{Static} = \frac{\mu_f}{(1 - \varphi)^{2.5}} \quad (13)$$

$$\frac{k_{static}}{k_f} = \frac{(k_p + 2k_f) - 2\varphi(k_f - k_p)}{(k_p + 2k_f) + \varphi(k_f - k_p)} \quad (14)$$

According to Koo- Kleinstreuer model (2004; 2005),  $\mu_{Brownian}$  and  $k_{Brownian}$  can be denoted as follows:

$$\mu_{Brownian} = 5 \times 10^4 \lambda \Phi \rho_f \sqrt{\frac{BT}{2\rho_{np}R_{np}}} f(T, \Phi) \quad (15)$$

$$k_{Brownian} = 5 \times 10^4 \lambda \Phi \rho_f c_{p,f} \sqrt{\frac{BT}{2\rho_{np}R_{np}}} f(T, \Phi) \quad (16)$$

Where  $\rho_{np}$  and  $R_{np}$  are the nanoparticles’ characteristics as density and radius respectively and  $B$  denotes Boltzmann number. Equations (17) - (19) are approximated For the CuO-water nanofluid experimentally:

$$\lambda = 0.0137(100\Phi)^{-0.8229} \text{ for } \Phi \leq 1\% \quad (17)$$

$$\lambda = 0.0011(100\Phi)^{-0.7272} \text{ for } \Phi > 1\% \quad (18)$$

And

$$f(T, \Phi) = (-6.04\Phi + 0.4705)T + (1722.3\Phi + 134.63) \quad (19)$$

for  $1\% \leq \Phi \leq 4\%$  and  $300K \leq T \leq 325K$

128 The wall boundary conditions in dimensionless form are as follow:

$$X = 0, \quad U = V = 0, \quad \theta = 1 \quad (20)$$

$$X = 1, \quad U = V = 0, \quad \theta = 0 \quad (21)$$

$$Y = 0, \quad Y = 1, \quad U = V = \frac{\partial \theta}{\partial Y} = 0 \quad (22)$$

129 Due to very slow velocity of nanofluid, it is considered that at boundaries of porous matrix the  
 130 tangential stresses and velocity in the nanofluid and porous media approximately identical  
 131 (Beckermann, 1987; Hadidi, 2016; Singh, 2011):

$$T_{nf} = T_{PM}, \quad k_{nf} \frac{\partial T}{\partial n} = k_{eff} \frac{\partial T}{\partial n} \quad (23)$$

$$U_{nf} = U_{PM}, \quad V_{nf} = V_{PM}, \quad P_{nf} = P_{PM} \quad (24)$$

$$\mu_{nf} \frac{\partial U_{nf}}{\partial n} = \mu_{eff} \frac{\partial U_{PM}}{\partial n}, \quad \mu_{nf} \left( \frac{\partial V_{nf}}{\partial n} + \frac{\partial U_{nf}}{\partial t} \right) = \mu_{eff} \left( \frac{\partial V_{PM}}{\partial n} + \frac{\partial U_{PM}}{\partial t} \right) \quad (25)$$

132 The nanofluid's Nusselt number is varied on the right and left boundaries according to equations  
 133 below (Oztop, 2008):

$$Nu_R = -\frac{k_{nf}}{k_f} \left( \frac{\partial \theta_{nf}}{\partial X} \right)_{X=1} \quad (26)$$

$$Nu_L = -\frac{k_{nf}}{k_f} \left( \frac{\partial \theta_{nf}}{\partial X} \right)_{X=0} \quad (27)$$

1  
2  
3 134 The net dimensionless heat generation of porous matrix is expressed by appending the local  
4  
5 135 Nusselt number over the right and left boundaries.

6  
7  
8  
9 
$$Nu = \int_0^1 (Nu_R + Nu_L) dY \tag{28}$$
  
10  
11

12 136 For numerical solving and discretization of the governing equation above, a control volume  
13  
14 137 technique was employed. A first order upwind method was used for the convective and diffusive  
15  
16 138 terms. While SIMPLE procedure was employed for the velocity-pressure coupling (Patankar,  
17  
18 139 1980).

21  
22  
23 140 **2.3 Grid independency and code validation**

24  
25 141 To assess independency of grid dimensions, different arrangement of grid dimensions were  
26  
27 142 investigated at the condition of  $Ra=10^5$ ,  $\epsilon=0.4$ ,  $R_k=10$  and  $q=1000$ . The average Nusselt number  
28  
29 143 for different grid sizes is presented in Table 2. As shown in table 2, results in the grid size of  
30  
31 144  $100 \times 100$  show less than 1% variance with the results in the grid size of  $120 \times 120$ . Therefore, to  
32  
33 145 keep a balanced trade-off between convergence time and solution accuracy, the adopted grid size  
34  
35 146 in the computational domain was  $100 \times 100$ .

36  
37  
38 147 It must be noted all the computational calculations were carried out by computer with  
39  
40 148 Processor: Intel-Core i3-3220 CPU @ 3.30GHZ, 4.00 GB Ram and 32-bit Operating System. Also  
41  
42 149 Fig.2 illustrates the residuals of continuity, momentum, and energy equations' solution. As can be  
43  
44 150 seen from this figure, the convergence of the results is smooth. Therefore it can be said that,  
45  
46 151 modeling this work in considered conditions and geometry is reliable.

47  
48  
49 152 Validation of the code was carried out in two steps. First, results obtained from the present work  
50  
51 153 for an enclosure partly filled with porous material were compared to the values obtained from the  
52  
53 154 Beckermann et al (1987). This comparison was conducted with conditions of  $Pr=1$ ,  $R_k=1$  and

C=0.55 and was shown in Fig. 3. It should be mentioned that the S reagent, the space which is not occupied with porous material along the x direction. Secondly, Nusselt number obtained from the present study for the cavity filled with CuO-water nanofluid were compared with the ones obtained from the Aminossadati and Ghasemi (2011). In Fig.4 it can be seen that the maximum difference between Nusselt number obtained in the present work and the data reported in Ref. (2011), in volume fraction of 0.02 and Rayleigh number of  $10^6$ , is about 0.9%.

### 3. Data processing

#### 3.1. Determining the effective value of interstitial heat transfer coefficient

Figure 5 shows the variation of Brownian Nusselt number with conduction ratios for different porosities. Tests were conducted at the condition of  $Ra=10^5$ ,  $\phi=0.04$ ,  $\epsilon=0.2$ ,  $q=1000$ , and  $H=10$ . At low convection coefficients (e.g.10), increasing the conduction ratio has no effect on temperature distribution and the internal heat generation and subsequently changes of this parameter has no effect on the Nusselt number. On the other side, because of lack of heat transferred between the porous matrix and nanofluid, and also due to the high temperatures of the matrix, the generated heat and the resulting Nusselt number would be extremely low. Thus, in order to clarify the effect of the porous matrix's material on the Nusselt number tests were conducted at the higher convection coefficient and the value of H has to be set to 100.

#### 3.2. The variation of Brownian according to conduction

The contours of streamlines and isotherms in different porosities were conducted at the condition of  $Ra=10^5$ ,  $\phi=0.04$ ,  $H=100$  and  $q=1000$ , with and without Brownian term. The change in Brownian Nusselt number in the various conduction and porosities is shown in Fig. 6. Due to Impermeability

of porous matrix in lower porosities, the only scheme for transfer of generated heat inside the porous matrix is conduction. Thus, variation of conduction ratio causes more heat transfer and a higher Nusselt number, consequently. Results show that the increment of Nusselt number is significantly proportional to increment of the conduction ratio. The further increment of porosity leads to further penetration of nanofluid inside the matrix. Therefore, the dominated regime changes from conduction to convection heat transfer. In this condition, the heat would be harvested from the porous matrix by convection of nanofluid. Hence Nusselt number will be high and approximately equal in all conduction ratios.

**Figures 7 and 8** show the comparison of the nanofluid streamlines and isotherms for the condition with and without Brownian term. As can be mentioned earlier, the Brownian term increases the viscosity of nanofluid, so this term affects the velocity and smoothness of streamlines. The Fig. 7 shows that considering this term causes more smooth streamlines while ignoring this term results in secondary circulation even in lower porosities. Figure 8 shows the isotherms for the condition with and without Brownian term and results were compared with each other. The higher values of gap among solid and dashed lines result in more Brownian effects. Presence of Brownian term enhances thermal conduction and temperature decrement of the porous matrix and bigger Nusselt number. The data reveals that in almost zero porosity (the exact value is 0.005) at the  $R_k=0.1$ , the Brownian term is low. Consequently the Brownian (solid) and non- Brownian (dashed) isotherms inside the matrix overlap each other. By augmenting the conduction ratio, the difference between Brownian and non- Brownian isotherms increases which is indicative of bigger Brownian term effects.

197 Nusselt factor ( $Nu_B/Nu_{WB}$ ) was specified as the Nusselt number in the presence of Brownian term  
198 ( $Nu_B$ ) to Nusselt number of the non-Brownian term ( $Nu_{WB}$ ) ratio. Fig. 9 shows the variation of  
199 Nusselt factor with conduction ratio for various porosities.

200 According to this fact that at approximately zero porosities, porous matrix is almost  
201 impermeable, generated heat is transferred to outside the block purely by the heat conduction.  
202 Hence the generated heat in low thermal conduction ratios does not pass to nonporous field.  
203 Also, the Brownian term of nanofluid is not affected which in this case the value of Nusslet  
204 factor is low. By more increment of conduction ratio, the heat is released from porous matrix and  
205 influences viscosity and thermal conduction of nanofluid therefore heat transfer and Nusselt  
206 factor are enhanced. By increasing porosity in lower range of  $R_k$  values, the temperature of  
207 matrix also remains high that results in higher Brownian term and Nusselt factor. By  
208 approaching  $\epsilon=1$  and the gradual removing of porous media, heat conduction is replaced by  
209 convection and as a result matrix temperature and consequently the Brownian term and Nusselt  
210 factor are decreased. The Nusselt factor for  $R_k=1$  surpasses corresponding value for  $R_k=10$  in  
211 middle range of porosity [0.2, 0.4] because of switching the dominated regime from conduction  
212 to convection. Finally it can be deduced that the mounting porous matrix into cavity full of  
213 nanofluid has significant effect on Brownian term value. This effect is more obvious in lower  
214 porosities specifically in a low conduction ratio. While in high margin value of porosity even  
215 neglecting the Brownian term can cause rational results.

### 216 3.3. The effect of Rayleigh number

217 Since Brownian term effect on conduction regime was significant, the effects of volume fraction of  
218 nanofluid and Rayleigh number were investigated in lower porosities at the condition of  $\epsilon=0.4$ ,

219  $R_k=1$ ,  $q=1000$  and  $H=100$ . Fig. 10 illustrates the Nusselt number variations versus volume  
220 fractions in different Rayleigh numbers. Results indicated that the increased Rayleigh number  
221 highly increased the Nusselt number in all volume fractions that can be attributed to the increased  
222 circulation velocity of the nanofluid inside the cavity and therefore more cooling of porous matrix.  
223 Increased volume fraction also resulted in higher Nusselt number.

224 Unlike the assumption of the homogenous nanofluid, in this state the increasing process of the  
225 Nusselt number would be reduced due to Brownian viscosity increase, especially in heat source  
226 region. For this reason, the growth of Nusselt number in Rayleigh number of  $10^4$  is higher than  
227 those of  $10^5$  and  $10^6$ , respectively, and similar results concerning behavior of nanofluid is reported  
228 by Aminossadati and Ghasemi (2011).

229 Variations of Nusslet factor related to different Rayleigh number and volume fractions were shown  
230 in Fig. 11. The highest Nusslet factor was seen to occur at Rayleigh number of  $10^4$  which was due  
231 to the dominant effect of Brownian thermal conductivity on viscosity in lower Rayleigh numbers.  
232 In higher Rayleigh number, the circulation velocity of the nanofluid and the viscosity effect was  
233 higher in creating resistance which resulted in decreasing Nusselt factor compared to lower  
234 Rayleigh numbers. Instead, the increase of volume fraction of nanofluid caused to increased  
235 Nusselt factor and this increase was higher in lower Rayleigh numbers.

236 In lower Rayleigh numbers, conduction was the dominant regime in the cavity. Therefore,  
237 increasing volume fraction resulted in the higher thermal conduction of the nanofluid which plays  
238 a more significant role in Nusselt factor increase. Although, by increasing Rayleigh numbers  
239 viscosity increases so it had no significant effect on heat transfer due to lower circulation velocity  
240 of the fluid. In high Rayleigh numbers, by increasing volume fraction the effect of the viscosity

241 was higher and conduction effect was decreased that lead to the decreased Nusselt factor growth  
242 compared to lower Rayleigh numbers.

#### 243 4. Conclusion

244 In the present study, effect of mounting heat generating porous matrix in a close cavity on the  
245 Brownian term of CuO-water nanofluid was studied numerically. Viscosity and Thermal  
246 conductivity of nanofluid were assumed to be consisting of a static component and a Brownian  
247 component that were functions of volume fraction of the nanofluid and temperature.

248 According to obtained results mounting the porous matrix caused to change the streamlines and  
249 isotherms on nanofluid saturated cavity and enhance the value of Brownian term. The heat  
250 conduction of porous matrix plays an important role on variation of Brownian term. Due to the  
251 heat trapped in low heat conduction of porous matrix, its temperature and Brownian term were  
252 raised. This fact resulted in the greatest value of Nusselt factor in this region. Also based on  
253 decrement of conduction effect, the Brownian impact dropped where neglecting this term has an  
254 insignificant influence. On the other hand the Brownian term must be considered in porous matrix  
255 with lower porosities and conduction ratio.

256 It is obvious from the result in lower Rayleigh number the Brownian term impact has more  
257 importance, but by increasing Rayleigh number and due to increment of nanofluid viscosity  
258 influence the value of Brownian term was dropped severely. This impact caused to higher Nusselt  
259 factor at lower Rayleigh numbers, and vice versa.

260 Increased volume fraction increased non-linear Nusselt number, i.e. the process of Nusselt number  
261 increment was decreased gradually which could be due to the increased Brownian viscosity and it  
262 has more significant effect when compared to the thermal conduction. Also, incorporation of



1  
2  
3  
4  
5  
6  
7  
8  
9  
10  
11  
12  
13  
14  
15  
16  
17  
18  
19  
20  
21  
22  
23  
24  
25  
26  
27  
28  
29  
30  
31  
32  
33  
34  
35  
36  
37  
38  
39  
40  
41  
42  
43  
44  
45  
46  
47  
48  
49  
50  
51  
52  
53  
54  
55  
56  
57  
58  
59  
60

porous matrix resulted in increased contribution of Brownian term into Nusselt number at all volume fractions.

**References**

Alsabery, A.I., Sheremet, M.A., Chamkha, A.J., and Hashim, I. (2017), “Conjugate natural convection of Al<sub>2</sub>O<sub>3</sub>-water nanofluid in a square cavity with a concentric solid insert using Buongiorno’s two-phase model”, *International Journal of Mechanical Sciences*, Vol. 136, pp. 200-219.

Alsabery, A. I., Saleh, H., Hashim, I., and Hussain, S. H. (2016),” Darcian Natural Convection in Inclined Square Cavity Partially Filled Between the Central Square Hole Filled with a Fluid and Inside a Square Porous Cavity Filled with Nanofluid”, *Journal of Applied Fluid Mechanics*, Vol. 9 No. 4, pp. 1763-1775.

Aminossadati, S.M. and Ghasemi, B. (2011), “Natural convection of CuO-water nanofluid in a cavity with two pairs of heat source–sink”, *International Communications in Heat and Mass Transfer* Vol.38, pp.672 –678.

Ammar I. Alsabery, Muneer, A. Ismael, Ali J. Chamkha and Ishak Hashim. (2018). “Mixed convection of Al<sub>2</sub>O<sub>3</sub>-water nanofluid in a double lid-driven square cavity with a solid inner insert using Buongiorno’s two-phase model”, *International Journal of Heat and Mass Transfer*, Vol. 119, pp. 939–961.

Atul Kumar Singh, Pratibha Agnihotri, Singh N.P. and Ajay Kumar Singh. (2011), “Transient and non-Darcian effects on natural convection flow in a vertical channel partially filled with porous medium: Analysis with Forchheimer–Brinkman extended Darcy model”, *International Journal of Heat and Mass Transfer*, Vol.54, pp.1111–1120.

- 293 Beckermann, C., Ramadhyani, S., Viskanta, R. (1987), "Natural convection Flow and heat transfer  
294 between a fluid layer and a porous layer inside a rectangular enclosure", *Journal of Heat Transfer*,  
295 Vol.109, pp.363-370.
- 296
- 297 Bin Kim, G., Min Hyun, J. and Sang Kwak, H. (2001), "Buoyant convection in a square cavity  
298 partially filled with a heat-generating porous medium", *Numerical Heat Transfer, Part A*. vol.40,  
299 pp.601- 618.
- 300
- 301 Brinkman, H. C. (1952), "The viscosity of concentrated suspensions and solutions", *Journal of*  
302 *Chemical Physics*, Vol.20, pp.571-581.
- 303
- 304 Choi, SU. and Eastman, JA. (1995), *Enhancing thermal conductivity of fluids with nanoparticles*.  
305 Argonne National Lab., IL (United States).
- 306
- 307 Ergun, S. (1952), "Fluid flow through packed columns", *Chemical Engineering Progress*. Vol.48,  
308 pp.89-94.
- 309
- 310 Hadidi, N. and Bennacer, R. (2016), "Three-dimensional double diffusive natural convection  
311 across a cubical enclosure partially filled by vertical porous layer", *International Journal of*  
312 *Thermal Sciences*, Vol.101, pp.143-157.
- 313
- 314 Hakan F.Oztop, and Eiyad Abu-Nada (2008), "Numerical study of natural convection in partially  
315 heated rectangular enclosures filled with nanofluids", *International Journal of Heat and Fluid*  
316 *Flow*, Vol.29, pp.1326-1336.
- 317
- 318 Ioan Pop, Mohammad Ghalambaz and Mikhail Sheremet, (2016) "Free convection in a square  
319 porous cavity filled with a nanofluid using thermal non equilibrium and Buongiorno  
320 models", *International Journal of Numerical Methods for Heat & Fluid Flow*, Vol. 26 No. 3/4,  
321 pp.671-69.
- 322

- 323 Khanafer, K., Vafai, K. and Lightstone, M. (2003), "Buoyancy-driven heat transfer enhancement  
324 in a two-dimensional enclosure utilizing nanofluid", *International Journal of Heat and Mass  
325 Transfer*, Vol.46, pp.3639-3653.
- 326
- 327 Koo, J. and Kleinstreuer, C. (2004), "A new thermal conductivity model for nanofluids", Vol.6,  
328 pp. 577–588.
- 329
- 330 Koo, J. and Kleinstreuer, C. (2005), "Laminar nanofluid flow in microheat-sinks", *International  
331 Journal of Heat and Mass Transfer*, Vol.48, pp.2652–2661.
- 332
- 333 Mansour, M. A., Ahmed, S. E. and Rashad, A. M. (2016), "MHD Natural Convection in a Square  
334 Enclosure using Nanofluid with the Influence of Thermal Boundary Conditions", *Journal of  
335 Applied Fluid Mechanics*, Vol. 9 No. 5, pp. 2515-2525.
- 336
- 337 Maxwell-Garnett, J. C. (1904), "Colours in metal glasses and in metallic films", *Philosophical  
338 Transactions of the Royal Society A*, Vol.203, pp.385–420.
- 339
- 340 Nield, D.A. and Kuznetsov, A.V. (2009), "Thermal instability in a porous medium layer saturated  
341 by a nanofluids", *International Journal of Heat and Mass Transfer*, Vol.52, pp.5796–5801.
- 342
- 343 Patankar, S.W. (1980), *Numerical Heat Transfer and Fluid Flow*. McGraw-Hill, NewYork.
- 344
- 345 Qiang Sun and Ioan Pop, (2013) "Free convection in a tilted triangle porous cavity filled with Cu-  
346 water nanofluid with flush mounted heater on the wall", *International Journal of Numerical  
347 Methods for Heat & Fluid Flow*, Vol. 24 No. 1, pp.2-20.
- 348
- 349 Rashad, A.M., Armaghani, T., Chamkha, A.J. and Mansour, M.A. (2018), "Entropy Generation  
350 and MHD Natural Convection of a Nanofluid in an Inclined Square Porous Cavity: Effects of a  
351 Heat Sink and Source Size and Location", *Chinese Journal of Physics*, Vol. 56, pp. 193-211.
- 352

- 353 Rashad, A.M., Rama Gorla, Mansour, M.A., Sameh E. Ahmed, (2017), "Magnetohydrodynamic  
354 effect on natural convection in a cavity filled with a porous medium saturated with nanofluid",  
355 *Journal of Porous Media*, Vol. 20 No.4, pp.363-379.
- 356
- 357 Rashad, A.M., Rashidi, M.M., Giulio Lorenzini, Sameh E. Ahmed and Abdelraheem M. Aly,  
358 (2017), "Magnetic field and internal heat generation effects on the free convection in a rectangular  
359 cavity filled with a porous medium saturated with Cu–water nanofluid", *International Journal of*  
360 *Heat and Mass Transfer*, Vol. 104, pp. 878–889.
- 361
- 362 Rashidi, M.M., Keimanesh, M. and Rajvanshi, S.C., (2012) "Study of pulsatile flow in a porous  
363 annulus with the homotopy analysis method", *International Journal of Numerical Methods for*  
364 *Heat & Fluid Flow*, Vol. 22 No. 8, pp.971-989.
- 365
- 366 Rashidi, M.M., Vishnu Ganesh, N., Abdul Hakeem, A.K. and Ganga, B. (2014), "Buoyancy Effect on  
367 MHD Flow of Nanofluid over a Stretching Sheet in the Presence of Thermal Radiation", *Journal of*  
368 *molecular Liquids*, Vol.198, pp. 234-238.
- 369
- 370 Rashidi, M.M., Mohimani pour, S.A. and Abbasbandy, S. (2011), "Analytic Approximate  
371 Solutions for Heat Transfer of a Micropolar Fluid through a Porous Medium with Radiation",  
372 *Communications in Nonlinear Science and Numerical Simulations*, Vol.16 No.4, pp.1874–1889.
- 373
- 374 Rashidi, M.M., Abelman, S., Freidoonimehr, N. (2013), "Entropy Generation in Steady MHD Flow  
375 Due to a Rotating Porous Disk in a Nanofluid", *International Journal of Heat and Mass Transfer*,  
376 Vol.62, pp.515–525.
- 377
- 378 Sameh Elsayed Ahmed, Rashad, A.M., (2016)," Natural convection of micropolar nanofluids in a  
379 rectangular enclosure saturated with anisotropic porous media", *Journal of Porous Media* , Vol. 19  
380 No.8, p.p. 737-750.
- 381

382 Sheikholeslami, M., Rashidi, M.M. and Ganji, D.D. (2015) “Effect of Non-uniform Magnetic Field on  
383 Forced Convection Heat Transfer of  $\text{Fe}_3\text{O}_4$ -Water Nanofluid”, *Computer Methods in Applied  
384 Mechanics and Engineering*, Vol. 294, pp. 299–312.  
385  
386 Sheremet, M. A. and Ioan Pop, (2015) "Free convection in a triangular cavity filled with a porous  
387 medium saturated by a nanofluid: Buongiorno’s mathematical model", *International Journal of  
388 Numerical Methods for Heat & Fluid Flow*, Vol. 25 No. 5, pp.1138-1161.  
389  
390 Teamah, M. A, El-Maghlany, W. M. (2012), “Augmentation of natural convective heat transfer in  
391 square cavity by utilizing nanofluids in the presence of magnetic field and uniform heat  
392 generation/absorption”, *International Journal of Thermal Sciences*, Vol.58, pp.130-142.  
393  
394

395 **Table1:** nanoparticle and fluid properties (Aminossadati et al. 2011)

396 **Table 2:** Average Nusselt number for different grid dimensions.

397  
398 **Fig.1.** Geometry of the problem

399 **Fig.3.** Comparison of the applied code with Beckermann (1987)

400 **Fig.4.** Comparison of the present code with Aminossadati and Ghasemi (2011)

401 **Fig.5.** Brownian Nusselt number for various  $R_k$  and  $\epsilon$  at  $H=10$

402 **Fig.6.** Nusselt number for various  $R_k$  and  $\epsilon$  at  $H=100$

403 **Fig.7.** Streamlines of Brownian (solid) and non-Brownian (dashed) cases

404 **Fig.8.** Isotherms of non-Brownian (dashed) and Brownian (solid) cases

405 **Fig.9.** Nusselt factor for various  $R_k$  and  $\epsilon$

406 **Fig.10.** Total Brownian Nusselt number for different  $Ra$  and  $\phi$

407 **Fig.11.** Nusselt factor for different  $Ra$  and  $\phi$

408

### Nomenclature

$c_p$	specific heat( J. kg <sup>-1</sup> . K <sup>-1</sup> )
$h$	convective heat transfer coefficient (W. m <sup>-2</sup> . K <sup>-1</sup> )
$K$	permeability of the porous medium (m <sup>2</sup> )
$k$	thermal conductivity (W. m <sup>-1</sup> . K <sup>-1</sup> )
$Q_0$	constant coefficient of heat generation (W. K. m <sup>-2</sup> )

### Greek symbols

$\alpha$	thermal diffusivity (m <sup>2</sup> . s)
$\beta$	thermal expansion coefficient, 1/K
$\lambda$	modeling function Eq. (21-22)
$\phi$	volume fraction of nanoparticles

### Subscripts

f	fluid
nf	nanofluid
p	nanoparticle
PM	Porous media
s	solid

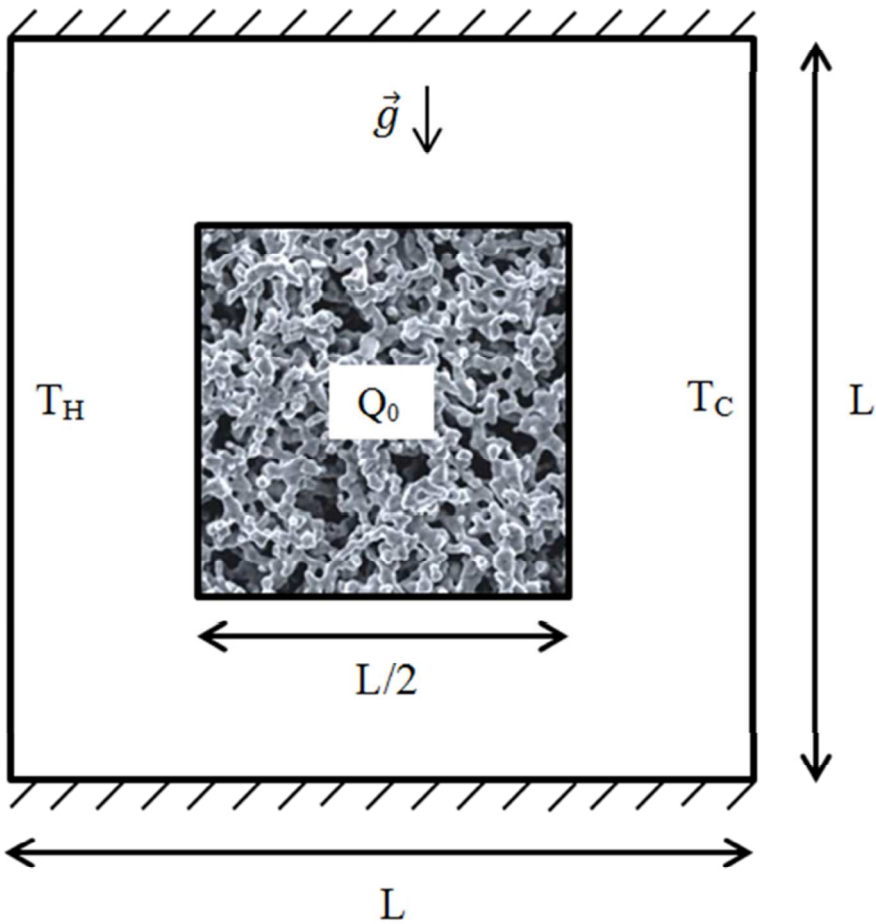


Fig.1. Geometry of the problem  
219x224mm (96 x 96 DPI)

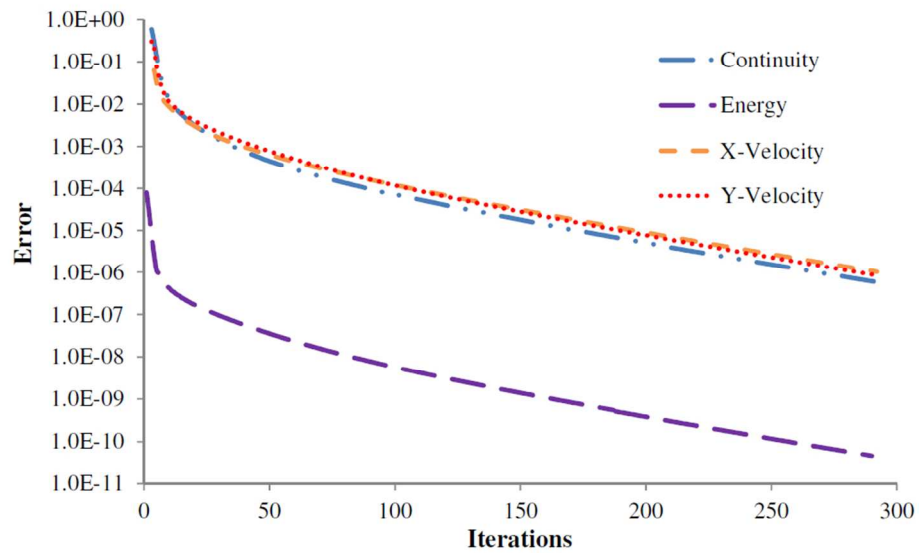


Fig.2 residuals of continuity, momentum, and energy equations' solution

287x175mm (96 x 96 DPI)



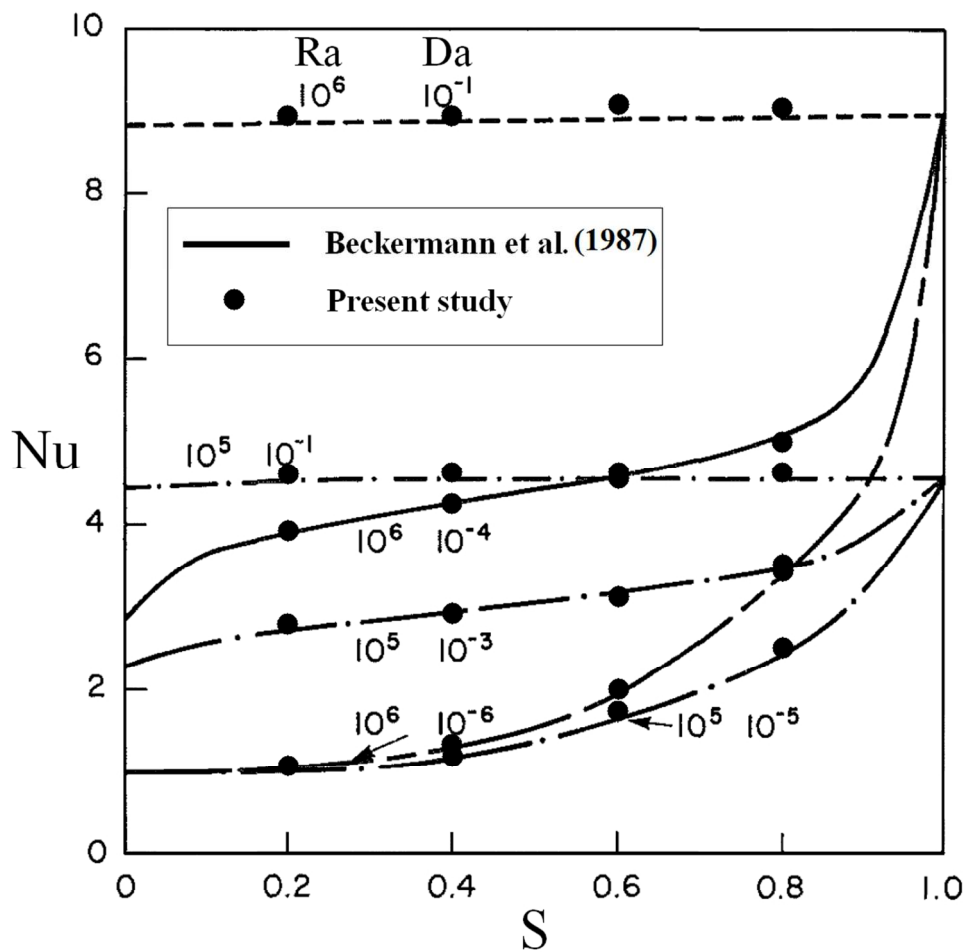


Fig.3. Comparison of the applied code with Beckermann (1987)

303x301mm (96 x 96 DPI)

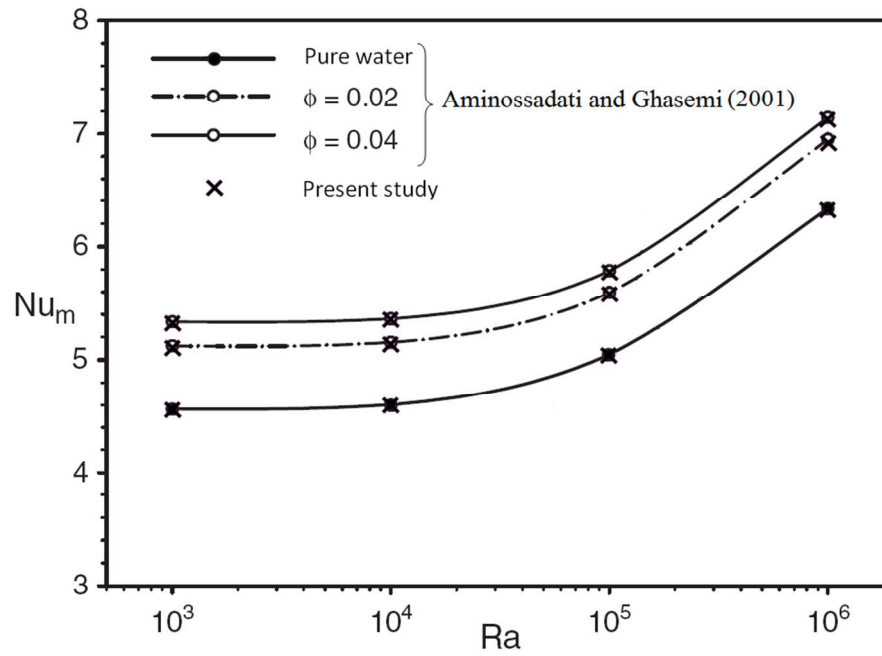


Fig.4. Comparison of the present code with Aminossadati and Ghasemi (2011)

290x198mm (96 x 96 DPI)

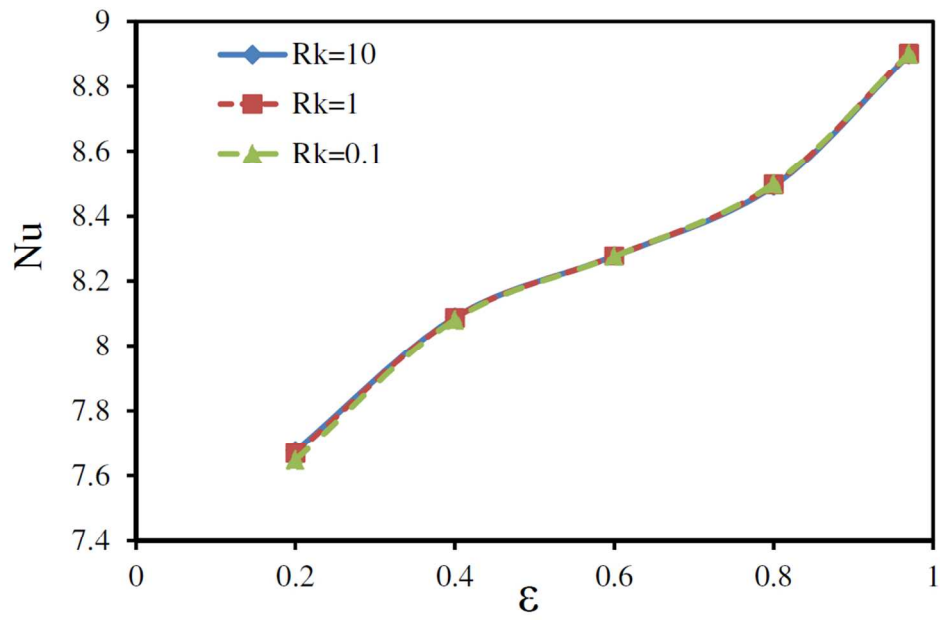


Fig.5. Brownian Nusselt number for various  $Rk$  and  $\epsilon$  at  $H=10$

316x206mm (96 x 96 DPI)

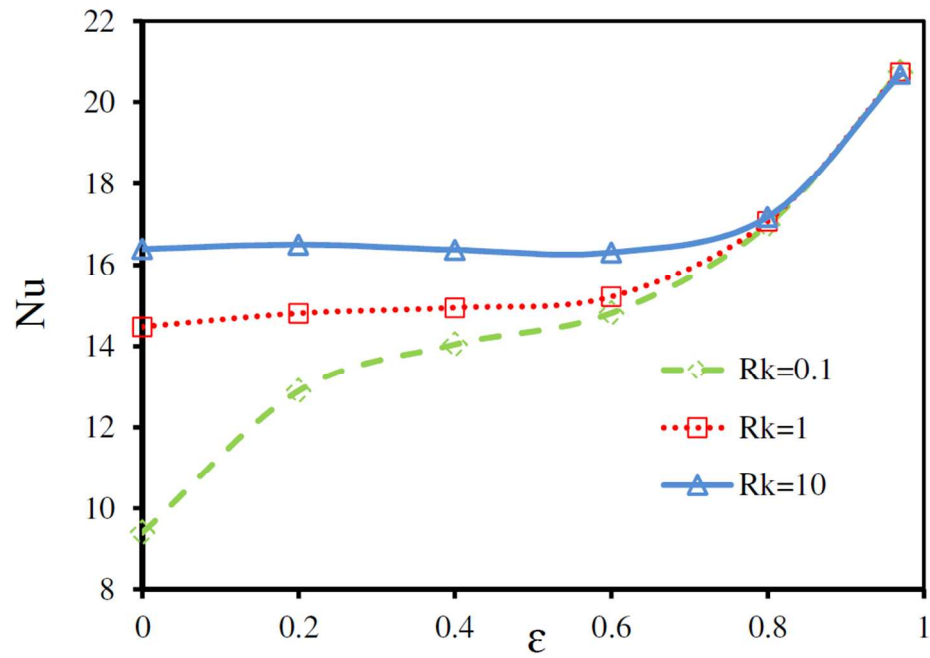


Fig.6. Nusselt number for various  $Rk$  and  $\epsilon$  at  $H=100$

303x209mm (96 x 96 DPI)

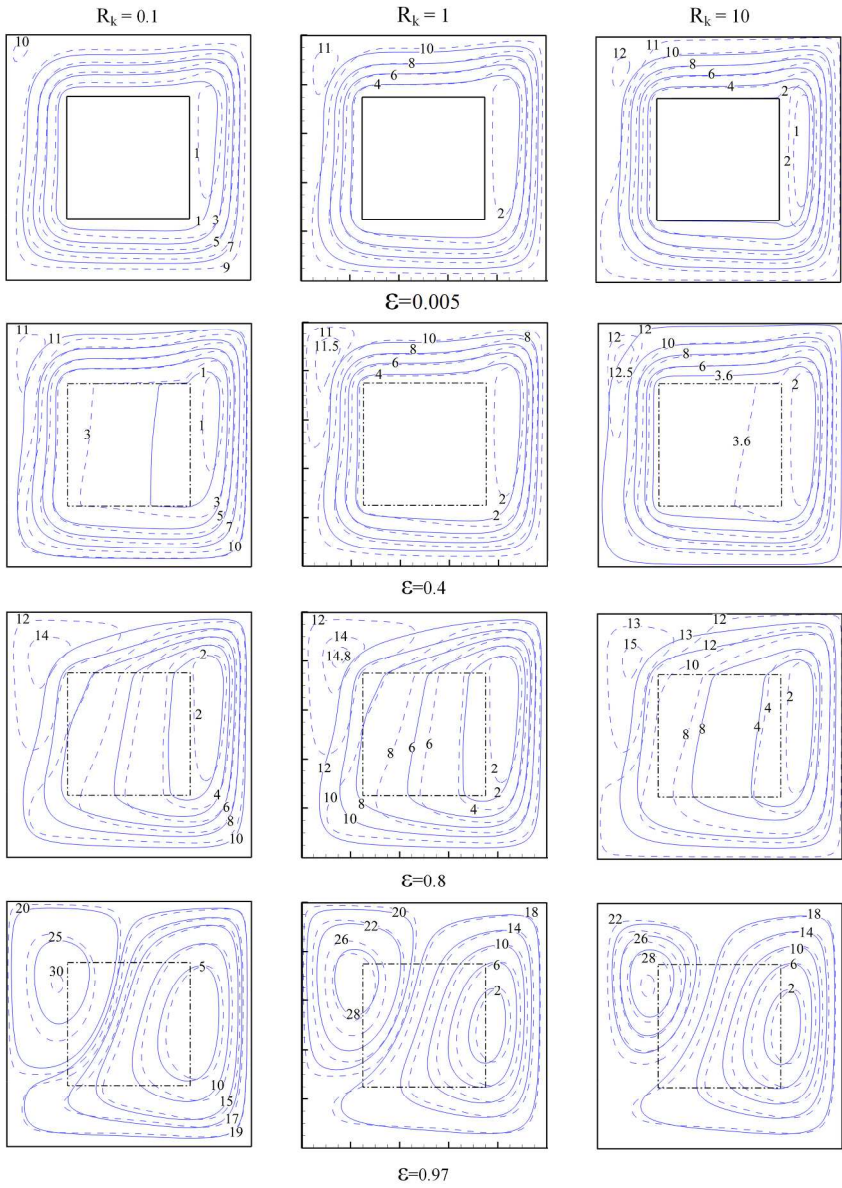


Fig.7. Streamlines of Brownian (solid) and non-Brownian (dashed) cases

652x841mm (101 x 101 DPI)

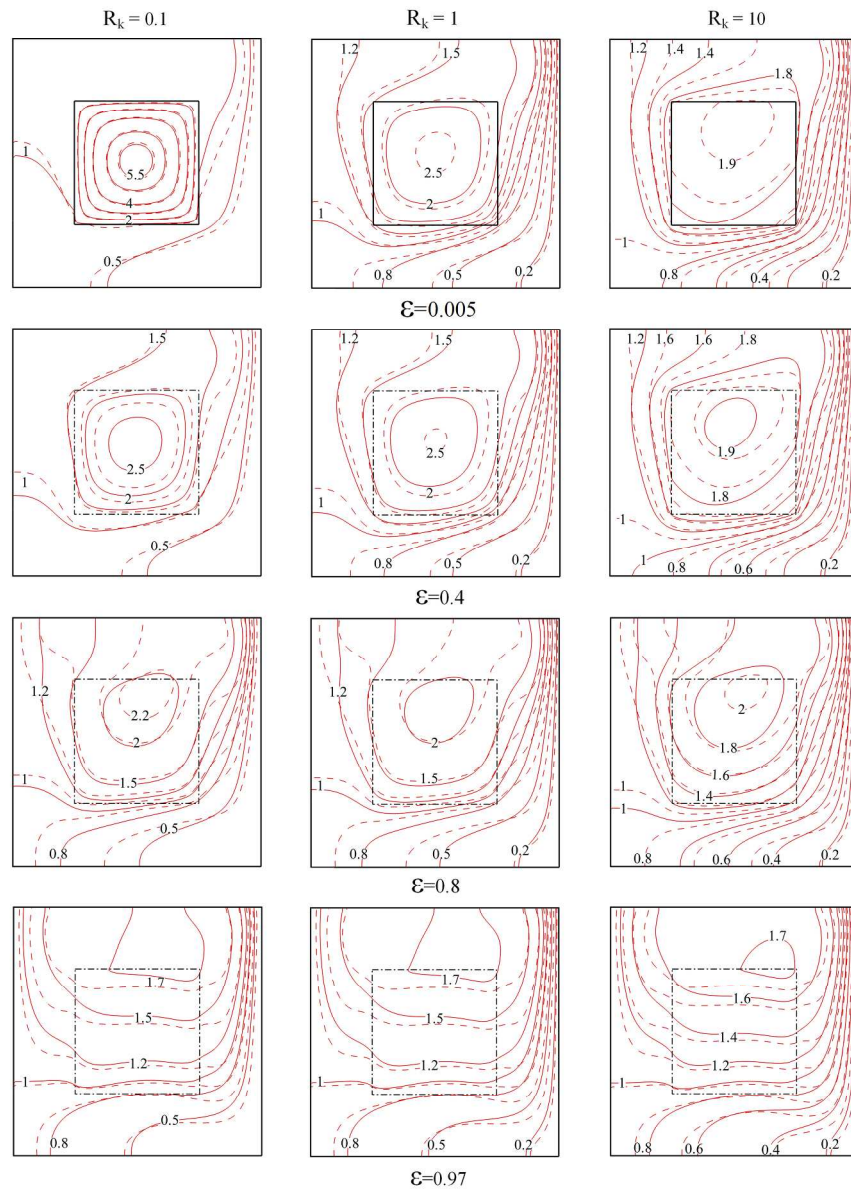


Fig.8. Isotherms of non-Brownian (dashed) and Brownian (solid) cases

686x873mm (96 x 96 DPI)

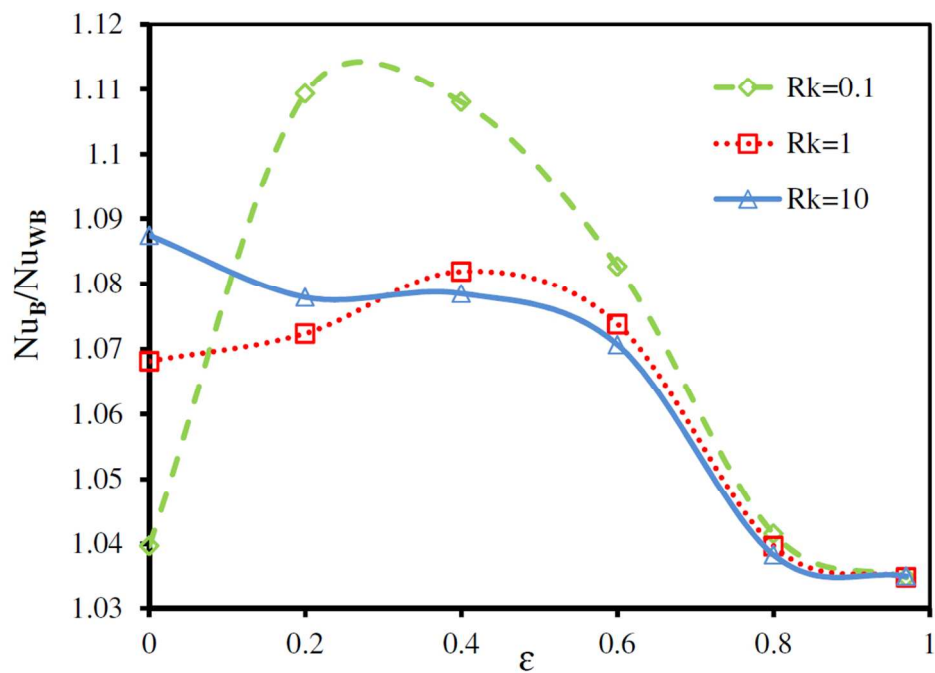


Fig.9. Nusselt factor for various  $Rk$  and  $\epsilon$

323x231mm (96 x 96 DPI)



Fig.10. Total Brownian Nusselt number for different  $Ra$  and  $\phi$

317x216mm (96 x 96 DPI)



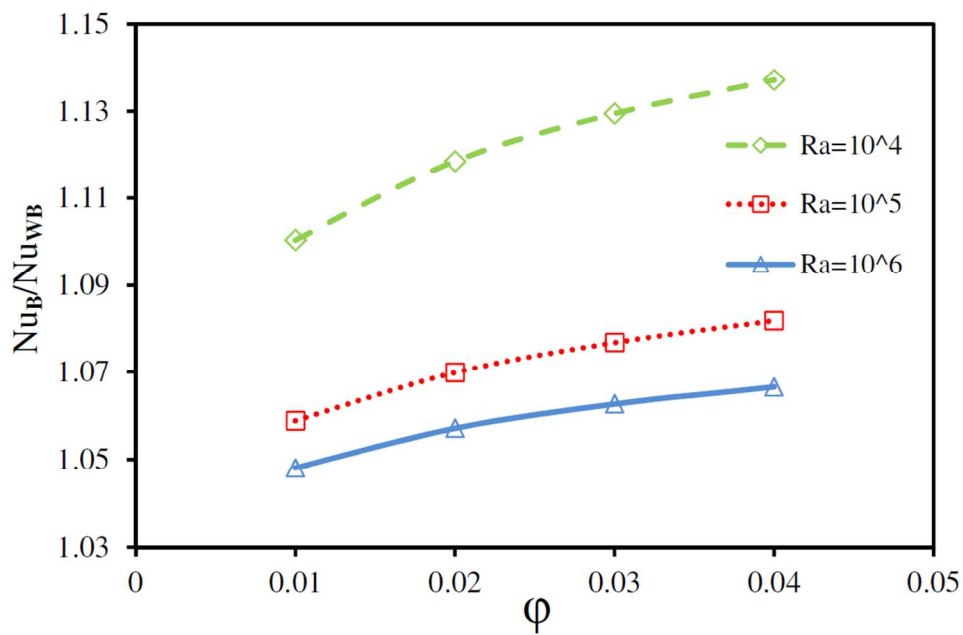


Fig.11. Nusselt factor for different Ra and  $\phi$

317x219mm (96 x 96 DPI)

	$\rho$	$\mu$	$c_p$	$k$	$\beta$
<b>water</b>	997.1	$8.81 \times 10^{-4}$	4179	0.613	$21 \times 10^{-5}$
<b>CuO</b>	6320	-	535.6	76.5	$1.8 \times 10^{-5}$

Table1: nanoparticle and fluid properties (Aminossadati et al. 2011)

225x97mm (96 x 96 DPI)

$\phi$	Grid dimensions	40×40	60×60	80×80	100×100	120×120
0.00	Nusselt number	15.2448	15.0757	14.9667	14.9071	14.9011
0.02		16.3184	16.1355	16.0653	16.0394	16.0349
0.04		16.7103	16.4758	16.4119	16.3755	16.3695

Table 2: Average Nusselt number for different grid dimensions.  
322x97mm (96 x 96 DPI)